On the Performance of Non-orthogonal Multiple Access Systems With Partial Channel Information

Zheng Yang, *Student Member, IEEE*, Zhiguo Ding, *Senior Member, IEEE*, Pingzhi Fan, *Fellow, IEEE*, and George K. Karagiannidis, *Fellow, IEEE*

***Abstract*—In this paper, a downlink single-cell non-orthogonal multiple access (NOMA) network with uniformly deployed users is considered and an analytical framework to evaluate its performance is developed. Particularly, the performance of NOMA is studied by assuming two types of partial channel state information (CSI). For the first one, which is based on *imperfect CSI*, we present a simple closed-form approximation for the outage probability and the average sum rate, as well as their high signal-to-noise ratio (SNR) expressions. For the second type of CSI, which is based on *second order statistics (SOS)*, we derive a closed-form expression for the outage probability and an approximate expression for the average sum rate for the special case two users. For the addressed scenario with the two types of partial CSI, the results demonstrate that NOMA can achieve superior performance compared to the traditional orthogonal multiple access (OMA). Moreover, SOS-based NOMA always achieves better performance than that with imperfect CSI, while it can achieve similar performance to the NOMA with perfect CSI at the low SNR region. The provided numerical results confirm that the derived expressions for the outage probability and the average sum rate match well with the Monte Carlo simulations.**

***Index Terms*—Non-orthogonal multiple access, imperfect channel state information, second order statistics, uniform distribution.**

I. Introduction

NON-ORTHOGONAL multiple access (NOMA) has been recognized as a promising candidate for the fifth generation (5G) wireless networks, since NOMA can be easily combined with multi-user multiple-input multiple-output (MU-MIMO) techniques, heterogeneous networks, small cells and networks with high mobility for significantly enhancing the system performance [1], [2]. On the other hand, downlink NOMA has been recently proposed to 3rd generation partnership project (3GPP)–long term evolution–advanced (LTE-A) systems [3], in order to improve the spectral efficiency in the lower frequency bands. The key concept behind NOMA is that users' signals are superimposed at the base station (BS) with different power allocation coefficients, and successive interference cancellation (SIC) is applied at the user with better channel condition, in order to remove the other users' signals before detecting its own signal [4]. Note that the concept of NOMA is a special case of the information theoretic concept of *superposition coding*. Moreover, it is worth pointing out that the key feature of NOMA is to take user fairness into consideration. For example, compared to conventional water-filling power allocation, NOMA allocates more power to users with worse channel conditions than those with better channel conditions, in order to realize an improved trade-off between system throughput and user fairness. As a result, all users share the same time slot, frequency and spreading code, which leads to an increase in spectral efficiency.

Manuscript received March 20, 2015; revised August 30, 2015 and December 9, 2015; accepted December 10, 2015. Date of publication December 22, 2015; date of current version February 12, 2016. The work of Z. Yang and P. Fan was supported by the National Science Foundation of China (NSFC, No. 61471302), the National Science and Technology Major Project (No. 2016ZX03001018-002), and the 111 Project (No. 111-2-14). The work of Z. Ding was supported by the UK EPSRC under grant number EP/L025272/1. The associate editor coordinating the review of this paper and approving it for publication was Z. Dawy.

Z. Yang and P. Fan are with the Institute of Mobile Communications, Southwest Jiaotong University, Chengdu 610031, China (e-mail: zyfjnu@163.com; p.fan@ieee.org).

Z. Ding is with the School of Computing and Communications, Lancaster University, Lancaster LA1 4YW, U.K. (e-mail: z.ding@lancaster.ac.uk).

G. K. Karagiannidis is with the Provincial Key Laboratory of Information Coding and Transmission, Southwest Jiaotong University, Chengdu 610031, China, and also with the Department of Electrical and Computer Engineering, Aristotle University of Thessaloniki, Thessaloniki GR-54124, Greece (e-mail: geokarag@auth.gr).

Color versions of one or more of the figures in this paper are available online at http://ieeexplore.ieee.org.

Digital Object Identifier 10.1109/TCOMM.2015.2511078

A. Literature and Motivation

In [5], a coordinated superposition coding scheme was presented, which can improve the cell-edge users' rate, without sacrificing the rate of the users who are close to the BS. Recently, the concept of cooperative NOMA has been proposed in [6], where users with better channel conditions need to decode the signals on behalf of others, and they can be used as relays to help the BS to communicate with users with poor channel conditions. In [7], the uplink communication of NOMA systems has been considered, while the impact of user pairing in NOMA systems over small-scale fading, with fixed and cognitive radio inspired power allocation, has been investigated in [8]. For the addressed single-antenna downlink NOMA scenario, superposition coding and dirty paper coding yield the same performance, and both achieve the capacity of the broadcasting channel [9]. As shown in [10], the use of NOMA can further improve the spectral efficiency of MIMO systems, e.g., users in one cell are divided into multiple groups, where MIMO technologies can be used to cancel inter-group interference and NOMA can be implemented among the users within one group. Furthermore, in [11], the outage probability and the average sum rate of downlink single-cell NOMA systems have been studied, by assuming that randomly deployed users are independently and identically distributed (i.i.d.) inside a disk,

i.e. the distribution of users follows a general binomial point process (BPP) [12]. Note that such an assumption it is true in real-world wireless networks [13], [14].

Recently, optimal power allocation based on average channel state information (CSI) has been considered in [15], by using the outage probability as the criterion, whereas the ergodic capacity of MIMO-NOMA systems with second order statistical (SOS) CSI at the transmitter has been studied in [16]. However, [15] and [16] focused on the case that user locations are fixed, i.e., distances and path loss are deterministic. Therefore, most of the existing works in the open literature about NOMA assume perfect knowledge of CSI. However, in practice, the assumption of perfect CSI at the transmitter might not be valid, since in order to obtain perfect CSI a significant system overhead will be consumed, especially in wireless network with a large number of users. Furthermore, towards 5G, there will be a growing demand for mobile services, such as serving users in high-speed trains, where due to the rapidly changing channel, perfect CSI at the transmitter is challenging to be achieved. Motivated by these practical constraints, we focus on the use of partial CSI, which is important to reduce the system complexity and improve the spectral efficiency of NOMA. Furthermore, we compare the results of NOMA with partial to the case with perfect CSI, which could help the system designers of NOMA.

In this paper, we consider a downlink single-cell NOMA network, where the users are uniformly distributed in a disk and the BS is located at the center. The impact of two types of partial CSI, named *imperfect CSI* and *SOS*, on the performance of NOMA is investigated. In particular, the two different types of partial CSI are defined as follows.

- *Imperfect CSI*: We assume the channel estimation error model presented in [17], [18], where the BS and the users have an estimate of the channel and a priori knowledge of the variance of the estimation error.
- *SOS*: Only the distances between the BS and the users are known. In a single-tier network, the distance varies much slower than the channel in small-scale fading conditions. Therefore, it is more realistic to assume the knowledge of the SOS of the wireless channels.

B. Contribution

The contribution of this paper is three-fold:

1) We investigate the impact of imperfect CSI on the performance of the NOMA network. More specifically, we focus on the minimum mean square error (MMSE) channel estimation error model. In such a scenario, a simple closed-form approximation for the outage probability is derived. Also, exact closed-form expressions for the outage probability are provided for the cases where the path loss exponent is two, as well for the NOMA systems based on perfect CSI with arbitrary path loss exponent. In addition, we study the high signal-to-noise ratio (SNR) outage behaviour and show that all users have a diversity order of zero, since the channel estimation error acts as a source of interference in the addressed system. However, for the special case with perfect CSI, the k-th best user achieves a diversity gain of $M-k+1$, where M is the number of users, which is superior to traditional orthogonal multiple access (OMA). Furthermore, an approximation of the average sum rate is also derived, and we use these analytical results to compare with the traditional OMA, which demonstrates that the average sum rate of NOMA systems can always outperform conventional OMA.

2) We derive an exact expression for outage probability in the case that the SOS of the channels is known. Since the channels are sorted accordingly by distances, order statistics of the distance is applied to yield closed-form expressions for the outage probability [19]. In addition, we find that all users in this scheme achieve a diversity gain of one, which is the same as in conventional OMA when CSI is also unknown. However, the former's outage performance is much better than the latter one for all users, even when the channels of OMA are also ordered by SOS. Moreover, an approximation for the average sum rate in the two users case is also obtained by using the Gauss-Chebyshev integration [20]. With the sum rate as criterion, SOS based NOMA is still superior to conventional OMA, which is consistent to the comparison based on the outage performance.

3) We present a comparison between the two different NOMA schemes, based on imperfect CSI and SOS, respectively. The presented analytical and numerical results demonstrate that SOS based NOMA always achieves better performance than that with imperfect CSI. Furthermore, the performance of the SOS based NOMA is similar to that with perfect CSI at low SNRs. This can be explained because large-scale path loss is dominant for most of the wireless communication scenarios.

C. Structure

The rest of the paper is organized as follows. Section II describes the system model. Section III studies the outage performance and the average sum rate of NOMA with imperfect CSI, while Section IV investigates the performance of NOMA systems based on SOS. In Section V, numerical results are presented and Monte Carlo simulations are applied to verify the accuracy of the proposed analysis. Finally, Section VI concludes the paper.

II. System Model

We consider a single-cell downlink wireless network in which the locations of M users are uniformly distributed in a disc with radius D, denoted by $\mathcal{D}$, and the BS is located at the center of the disc. It is assumed that all users are served by the same orthogonal channel use, which can be a time slot, a spreading code or a frequency channel. Furthermore, assume that all the users and the BS are equipped with a single antenna. The channel between user U_i and the BS is denoted by $r_i = h_i / d_i^{\frac{\alpha}{2}}$, where $h_i \sim \mathcal{CN}(0,1)$ with $\mathcal{CN}(a,b)$ is the complexed Gaussian distribution with mean a and variance b, d_i is the distance between the BS and the user U_i, and α is the path loss exponent. It is well known that the optimal system performance can be achieved with perfect CSI. However, to obtain instantaneous perfect CSI, the backhaul signalling overhead

increases significantly, which, consequently, will then increase the system complexity. Based on this fact, in this paper we consider two types of practical channel models: imperfect CSI and SOS. The two different NOMA systems based on these models are described as follows.

A. NOMA Based on Imperfect CSI

In this paper, we assumed that the feedback to the transmitter is instantaneous and error free, which means that CSI is also achievable at the transmitter whatever CSI the receiver has. Note that this assumption has been commonly used in the literature [17], [18], [21]–[23]. Let the estimate for the channel r_k be $\hat{r}_k$. By assuming MMSE estimation error, it holds that [21]–[23]

$$r_k = \hat{r}_k + \epsilon, \tag{1}$$

where ϵ is the channel estimation error, which follows a complex Gaussian distribution with mean 0 and variance σ_ϵ^2, denoted by $\epsilon \sim \mathcal{CN}(0, \sigma_\epsilon^2)$. The channel estimate $\hat{r}_k$ is thus zero-mean complex Gaussian with variance $\sigma_{\hat{r}_k}^2 = d_k^{-\alpha} - \sigma_\epsilon^2$ [21]–[23]. Note that the parameter σ_ϵ^2 indicates the quality of channel estimation.

Without loss of generality, assume that the estimated channel gain in the cell are sorted as $|\hat{r}_1|^2 \geq |\hat{r}_2|^2 \geq \cdots \geq |\hat{r}_M|^2$, and denote the corresponding users as $U_1, \ldots, U_M$. According to NOMA scheme, the signal s_l ($l = 1, 2, \cdots, M$), sent by the BS to the user U_l ($l = 1, 2, \cdots, M$) is superimposed as

$$x = \sum_{l=1}^{M} \sqrt{\alpha_l P} s_l,$$

where P is the transmission power, and α_l ($l = 1, 2, \cdots, M$) is the power allocation factor, with $\alpha_1 < \alpha_2 < \cdots < \alpha_M$ and $\sum_{l=1}^{M} \alpha_l = 1$. Therefore the received signal at user U_k in the cell $\mathcal{D}$ can be formulated as

$$y_k = \hat{r}_k \sum_{l=1}^{M} \sqrt{\alpha_l P} s_l + \epsilon \sum_{l=1}^{M} \sqrt{\alpha_l P} s_l + w_k, \tag{2}$$

where w_k is zero-mean additive white Gaussian noise (AWGN) with variance σ^2.

Based on (2), SIC can be employed at U_k. In other words, U_k needs to detect firstly the message s_l to the user U_l ($M \geq l \geq k+1$), before decoding its own signal. For example, the data rate for U_k to decode the message to the user U_M is $R_{M\to k} = \log_2\left(1 + \frac{\alpha_M |\hat{r}_k|^2}{|\hat{r}_k|^2 \sum_{j=1}^{M-1} \alpha_j + \sigma_\epsilon^2 + \frac{1}{\rho}}\right)$. If U_k can decode this message successfully, i.e., $R_{M\to k} \geq R_M^*$, where R_M^* denotes the targeted rate of user U_M, then the signal s_M can be removed at U_k. After that, U_k can detect the signal from U_l ($M > l \geq k+1$), step by step, until U_k can correctly decode the signal s_{k+1}, for user U_{k+1}. The general rate expression for U_k to detect the signal U_l, $M \geq l \geq k+1$ is given by

$$R_{l\to k} = \log_2\left(1 + \frac{\alpha_l |\hat{r}_k|^2}{|\hat{r}_k|^2 \sum_{j=1}^{l-1} \alpha_j + \sigma_\epsilon^2 + \frac{1}{\rho}}\right). \tag{3}$$

Now, assuming that the user U_k decodes always correctly the message of user U_l, $k+1 \leq l \leq M$, the rate of user U_k can be expressed as

$$R_k = \log_2\left(1 + \frac{\alpha_k |\hat{r}_k|^2}{|\hat{r}_k|^2 a_{k-1} + \sigma_\epsilon^2 + \frac{1}{\rho}}\right), k = M, \ldots, 3, 2, \tag{4}$$

where $a_{k-1} = \sum_{l=1}^{k-1} \alpha_l$, $\rho = \frac{P}{\sigma^2}$ is the transmit SNR, and $R_1 = \log_2\left(1 + \frac{\alpha_1 |\hat{r}_1|^2}{\sigma_\epsilon^2 + \frac{1}{\rho}}\right)$.

B. NOMA Based on SOS

Let the k-th nearest user to the BS be indexed as U_k ($k = 1, 2, \cdots, M$), and the corresponding distance is denoted as d_k. Here we assume that the SOS is known, and the distances are sorted as follows: $d_1 \leq d_2 \leq \cdots \leq d_M$. A composite channel model is assumed, defined by small-scale Rayleigh fading and large-scale path loss. Note that the channel gain is $|r_k|^2 = |h_k|^2 d_k^{-\alpha}$, where $X = d_k^{-\alpha}$ is a *heavy tail* random variable (RV) such that

$$\Pr\{X > x\} = x^{\frac{-2}{\alpha}} / R^2, \tag{5}$$

since the users are uniformly distributed in the disk. Suppose that a heavy tail RV is multiplied by a RV, $Y = |h_k|^2$, with finite moments, i.e., $\mathrm{E}\{Y^{\frac{2}{\alpha}}\} < \infty$. Then

$$\Pr\{XY > z\} = \mathrm{E}\left\{Y^{\frac{2}{\alpha}}\right\} \frac{z^{\frac{-2}{\alpha}}}{R^2} \left(1 + o(1)\right), z \to \infty. \tag{6}$$

Compare (5) to (6), we can observe that the small-scale fading, Y, only weekly changes the large-scale fading X [24]. This is the motivation why we order the users based on their distances.

It is important to point out that the composite channel gains, r_k, are not necessarily ordered, i.e., r_j might be larger than r_k for $j > k$. Based on the NOMA protocol, the received signal at user U_k in the cell $\mathcal{D}$ is given as

$$y_k = r_k \sum_{l=1}^{M} \sqrt{\alpha_l P} s_l + w_k. \tag{7}$$

Similar to NOMA with imperfect CSI, denote $R'_{l\to k}$ as the rate of the k-th nearest user U_k to detect the message from the the l-th nearest user U_l. Assume that the U_k can decode the signal from U_l for $k < l$ successfully, i.e., $\Pr\left\{R'_{l\to k} \geq R_l^*\right\} = 1$, where

$$R'_{l\to k} = \log_2\left(1 + \frac{\alpha_l |r_k|^2}{|r_k|^2 \sum_{j=1}^{l-1} \alpha_j + \frac{1}{\rho}}\right). \tag{8}$$

If $\Pr\left\{R'_{l\to k} \geq R_l^*\right\} = 1$ holds for all $k < l$, then the rate of the k-th nearest user U_k can be expressed as

$$R_k = \log_2\left(1 + \frac{\alpha_k |r_k|^2}{|r_k|^2 a_{k-1} + \frac{1}{\rho}}\right), k = M, \ldots, 3, 2, \tag{9}$$

and $R_1 = \log_2\left(1 + \rho \alpha_1 |r_1|^2\right)$.

III. Performance of NOMA With Imperfect CSI

In this section, we study the outage performance and the average sum rate of NOMA systems with imperfect CSI. Outage probability is a measure of the event that the data rate supported by instantaneous channel realizations is less than a targeted user rate. Therefore, it is an important performance metric of the quality of service (QoS) in delay-sensitive communications, where the information is sent by the transmitter at a fixed rate, and the network throughput is defined as the coverage probability times the fixed rate.

Detection error events can be categorized into two cases: The first corresponds to an error detection when outage does not occur, and the second to an error detection when outage occurs. By using optimal coding with infinite length, the probability of the former approaches zero, and the latter is dominant [25]. This is another motivation to use in this paper the outage probability for performance evaluation process. On the other hand, the average data rate can be used for the case where the transmitted data rates are determined adaptively, according to the users' channel conditions. This case corresponds to delay-tolerant communications. Note that to obtain the outage performance and the average sum capacity, we assume optimal channel coding and modulation. The design of practical coding and modulation schemes is a promising future direction, but it is beyond the scope of this paper.

A. Outage Probability

The following Theorem provides an approximate expression for the outage probability of NOMA systems for the whole range of SNR and arbitrary path loss factor, with channel estimation error.

Theorem 1: The outage probability of the k-th user achieved by the NOMA scheme, assuming imperfect CSI, can be approximated as

$$\mathrm{P}_{out,I}^{k} \approx k\binom{M}{k}\sum_{r=0}^{k-1}\frac{\binom{k-1}{r}(-1)^r}{r+M-k+1}\left(1-\frac{\pi}{nD}\sum_{i=1}^{n}x_i \times\left|\sin\frac{2i-1}{2n}\pi\right|\exp\left(\frac{-\vec{\eta}(\rho\sigma_\epsilon^2+1)}{x_i^{-\alpha}-\sigma_\epsilon^2}\right)\right)^{r+M-k+1}, \quad (10)$$

where $x_i=\frac{D}{2}(1+\cos\frac{2i-1}{2n}\pi)$, n is an approximation parameter due to the use of the Gauss-Chebyshev integration, $\vec{\eta}=\max_{k+1\le i\le M}\eta_i$, $\eta_i=\frac{\varepsilon_i}{\rho\left(\alpha_i-\varepsilon_i\sum_{l=1}^{i-1}\alpha_l\right)}$, $\alpha_i>\varepsilon_i\sum_{l=1}^{i-1}\alpha_l$, and $\varepsilon_i=2^{R_i^*}-1$, R_i^* denotes targeted date rate of user U_i.

Proof: See Appendix A. ■

Note that n is an important parameter in (10), which affects the accuracy of the analytical results. As shown by the simulations provided in Section V, Gaussian-Chebyshev integration can achieve an accurate approximation even with a small number of n. In addition, the constraint, $\alpha_i>\varepsilon_i\sum_{l=1}^{i-1}\alpha_l$, is required in (10). However, because of the strong co-channel interference, a NOMA system is interference limited, i.e., the achievable data rates for some users will be quite small, which is applicable to many applications related to the Internet of Things (IoT). For example, some of the users, such as healthcare sensors or smart meters, need to be served only with low date rates. In this case, NOMA can be applied to serve these users at the same time, and thus to significantly improve the spectral efficiency. Note that if the users' power allocation coefficients are optimized according to instantaneous channel conditions, the performance can be further enhanced [15], but this is also beyond the scope of this paper.

In addition, the outage performance achieved by NOMA with imperfect CSI can be evaluated through Theorem 1 without carrying out Monte Carlo simulations. However, although (10) is consisting of elementary functions, it can not be used to investigate the diversity gain. Motivated by this, the high SNR approximation of the outage probability in (10) is provided in the following Proposition.

Proposition 1: In the high SNR region, i.e., $\rho\to\infty$, then $\vec{\eta}\to 0$, the outage probability achieved by NOMA with imperfect CSI, i.e., $\sigma_\epsilon^2\neq 0$, can be approximated as

$$\mathrm{P}_{out,I}^{k,\infty} \approx k\binom{M}{k}\sum_{r=0}^{k-1}\frac{\binom{k-1}{r}(-1)^r}{r+M-k+1}\left(1-\frac{\pi}{nD}\sum_{i=1}^{n}x_i \times\left|\sin\frac{2i-1}{2n}\pi\right|\exp\left(\frac{-\vec{c}\sigma_\epsilon^2}{x_i^{-\alpha}-\sigma_\epsilon^2}\right)\right)^{r+M-k+1}, \quad (11)$$

where $\vec{c}=\max_{k+1\le i\le M}\frac{\varepsilon_i}{\left(\alpha_i-\varepsilon_i\sum_{l=1}^{i-1}\alpha_l\right)}$.

Proof: When $\vec{\eta}\to 0$ and $\sigma_\epsilon^2\neq 0$, it holds that

$$\exp\left(\frac{-\vec{\eta}(\rho\sigma_\epsilon^2+1)}{x_i^{-\alpha}-\sigma_\epsilon^2}\right)\approx\exp\left(\frac{-\vec{c}\sigma_\epsilon^2}{x_i^{-\alpha}-\sigma_\epsilon^2}\right). \quad (12)$$

Substituting (12) into (10), (11) is derived. ■

Proposition 1 demonstrates that with imperfect CSI, the users in NOMA systems achieve no diversity gain, which is due to the fact that the channel estimation error acts as an interference source and significantly affects the outage performance.

For the special case, where the path loss exponent is, $\alpha=2$, we can obtain a closed-form expression for the outage probability as follows.

Corollary 1: When $\alpha=2$, the outage probability of the k-th user is given by

$$\mathrm{P}_{out,I}^{k,\alpha=2} = k\binom{M}{k}\sum_{r=0}^{k-1}\frac{\binom{k-1}{r}(-1)^r}{r+M-k+1}\left[1+\frac{\exp\left(-\frac{\vec{\eta}(\rho\sigma_\epsilon^2+1)}{\sigma_\epsilon^2}\right)}{D^2\sigma_\epsilon^2} \times\left(\exp\left(\frac{\vec{\eta}(\rho\sigma_\epsilon^2+1)}{\sigma_\epsilon^2}\right)-\exp\left(\frac{\vec{\eta}(\rho\sigma_\epsilon^2+1)}{\sigma_\epsilon^2(1-\sigma_\epsilon^2D^2)}\right)\right. \times(1-\sigma_\epsilon^2D^2)+\frac{\vec{\eta}(\rho\sigma_\epsilon^2+1)}{\sigma_\epsilon^2}\mathrm{Ei}\left(\frac{\vec{\eta}(\rho\sigma_\epsilon^2+1)}{\sigma_\epsilon^2(1-\sigma_\epsilon^2D^2)}\right) \left.-\frac{\vec{\eta}(\rho\sigma_\epsilon^2+1)}{\sigma_\epsilon^2}\mathrm{Ei}\left(\frac{\vec{\eta}(\rho\sigma_\epsilon^2+1)}{\sigma_\epsilon^2}\right)\right)\Bigg]^{r+M-k+1}, \quad (13)$$

where $\mathrm{Ei}(x)$ is the exponential integral [26].

Proof: When $\alpha = 2$, let $t = \frac{zx^2}{1-\sigma_\epsilon^2 x^2} - \frac{z}{\sigma_\epsilon^2}$, then the integral I in (34) can be rewritten as

$$\begin{aligned} I &= \int_0^D x \exp\left(\frac{-z}{x^{-2}-\sigma_\epsilon^2}\right) dx \\ &= \frac{ze^{-\frac{z}{\sigma_\epsilon^2}}}{2\sigma_\epsilon^4} \int_{-\frac{z}{\sigma_\epsilon^2}}^{-\frac{z}{\sigma_\epsilon^2(1-\sigma_\epsilon^2 D^2)}} \frac{e^{-t}}{t^2} dt \\ &= \frac{e^{-\frac{z}{\sigma_\epsilon^2}}}{2\sigma_\epsilon^2} \left((1-\sigma_\epsilon^2 D^2) \exp\left(\frac{z}{\sigma_\epsilon^2(1-\sigma_\epsilon^2 D^2)}\right) \right. \\ &\quad \left. - \exp\left(\frac{z}{\sigma_\epsilon^2}\right)\right) - \frac{ze^{-\frac{z}{\sigma_\epsilon^2}}}{2\sigma_\epsilon^4} \underbrace{\int_{-\frac{z}{\sigma_\epsilon^2}}^{-\frac{z}{\sigma_\epsilon^2(1-\sigma_\epsilon^2 D^2)}} \frac{e^{-t}}{t} dt}_{U}. \end{aligned} \quad (14)$$

Integral U can be evaluated as [26]

$$\begin{aligned} U &= \int_{-\frac{z}{\sigma_\epsilon^2}}^{\infty} \frac{e^{-t}}{t} dt - \int_{-\frac{z}{\sigma_\epsilon^2(1-\sigma_\epsilon^2 D^2)}}^{\infty} \frac{e^{-t}}{t} dt \\ &= \mathrm{Ei}\left(\frac{z}{\sigma_\epsilon^2(1-\sigma_\epsilon^2 D^2)}\right) - \mathrm{Ei}\left(\frac{z}{\sigma_\epsilon^2}\right). \end{aligned} \quad (15)$$

Substituting (14), (15) and (34) into (32), the proof is completed. ■

Note that the case with perfect CSI is also worth studying, since it provides a performance upper bound for that with partial CSI, where the loss due to imperfect CSI can be clearly demonstrated. If perfect CSI is available, a closed-form expression for the outage probability can be derived in the following Corollary.

Corollary 2: When $\sigma_\epsilon^2 = 0$, i.e., with perfect CSI, the outage probability of the k-th best user in NOMA systems is given by

$$\begin{aligned} \mathrm{P}_{out,I}^{k,\sigma_\epsilon^2=0} &= \sum_{r=0}^{k-1} \frac{k\binom{M}{k}\binom{k-1}{r}(-1)^r}{r+M-k+1} \\ &\quad \times \left(1 - \frac{2}{\alpha D^2 \vec{\eta}^{\frac{2}{\alpha}}} \gamma\left(\frac{2}{\alpha}, \vec{\eta} D^\alpha\right)\right)^{r+M-k+1}, \end{aligned} \quad (16)$$

where $\gamma(a, b)$ is a lower incomplete gamma function [26].

Proof: When $\sigma_\epsilon^2 = 0$,

$$\begin{aligned} F_{|\bar{r}_k|^2}(z) &= 1 - \frac{2}{D^2} \int_0^D x e^{-zx^\alpha} dx \\ &= 1 - \frac{2}{\alpha D^2 z^{\frac{2}{\alpha}}} \gamma(\frac{2}{\alpha}, zD^\alpha). \end{aligned} \quad (17)$$

Using (17) and (32) in Appendix A, the proof is completed. ■

Note that the outage performance of NOMA with perfect CSI has been already studied in [11], where an exact closed-form analytical result was presented, based on high SNR approximation. Compared to this result, the expression in (17) is more accurate for the whole range of SNR. This is because we use the exact expression for the cumulative distribution function (CDF) of the unordered composite channel gain, instead of its approximation, which is used in [11].

Proposition 2: In the high SNR region, i.e., $\rho \to \infty$, then $\vec{\eta} \to 0$, the outage probability achieved by NOMA with perfect CSI, i.e., $\sigma_\epsilon^2 = 0$, can be approximated as

$$\mathrm{P}_{out,I}^{k,\infty,\sigma_\epsilon^2=0} \approx k\binom{M}{k} \sum_{r=0}^{k-1} \frac{\binom{k-1}{r}(-1)^r}{r+M-k+1} \left(\frac{2D^\alpha \vec{\eta}}{\alpha+2}\right)^{r+M-k+1}. \quad (18)$$

Proof: When $\vec{\eta} \to 0$ and $\sigma_\epsilon^2 = 0$, the second term in (16) can be rewritten as [26]

$$\frac{2}{\alpha D^2 z^{\frac{2}{\alpha}}} \gamma(\frac{2}{\alpha}, \vec{\eta} D^\alpha) = 1 + \frac{2}{\alpha} \sum_{q=1}^{\infty} \frac{(-1)^q \vec{\eta}^q D^{\alpha q}}{q!(\frac{2}{\alpha}+q)}. \quad (19)$$

Substituting (19) into (16), the proof is completed. ■

Proposition 2 can be used to study the diversity gain, since (18) can be expressed as

$$\mathrm{P}_{out,I}^{k,\infty,\sigma_\epsilon^2=0} \approx A\rho^{-(M-k+1)}, \quad (20)$$

where A is a constant and the k-th best user achieves a diversity gain of $M-k+1$. Note that the users in NOMA systems achieve better diversity gain than those in traditional opportunistic OMA, with diversity order of one. This happens because the bandwidth resources in NOMA are shared by all users at the same time slot, which enhances the spectral efficiency and users fairness.

B. Average Sum Rate

In this subsection, we turn our attention to the average sum rate of NOMA systems with imperfect CSI. The Gauss-Chebyshev integration technique is applied to achieve a high level of accuracy for the whole range of SNR and arbitrary path loss factor.

Theorem 2: An approximation to the average sum rate of the NOMA protocol with imperfect CSI, is given by (21) shown at the bottom of the next page, where the summation is taken over all sequences of nonnegative integer indices t_1 through t_n, such that the sum of all t_i is j, $h(z) = \exp\left(\frac{1+\rho\sigma_\epsilon^2}{\rho z} \sum_{i=1}^n \frac{t_i}{x_i^{-\alpha}-\sigma_\epsilon^2}\right) \mathrm{E}_1\left(\frac{1+\rho\sigma_\epsilon^2}{\rho z} \sum_{i=1}^n \frac{t_i}{x_i^{-\alpha}-\sigma_\epsilon^2}\right)$, and $z = a_{k-1}, a_k$.

Proof: See Appendix B. ■

Compared to Monte Carlo simulations, the approximation for the average sum rate provided in Theorem 2 can offer a simpler way to evaluate the average sum rate in NOMA systems. The special case with perfect CSI, has been considered in [11], but the offered closed-form expression is accurate at only high SNRs. The reason is that firstly the Gauss-Chebyshev integration was applied to approximate the probability distribution function (PDF) of the unordered channel gain, and then the average sum rate was obtained at high SNRs. On the other hand, (21) is accurate even in low and moderate SNRs. This is because we obtain the exact expression for the PDF of the unordered channel gain, and then the Gaussian-Chebyshev integration is used to approximate the average sum rate, which yields much more accurate results.

For the special case of NOMA with perfect CSI, i.e., $\sigma_\epsilon^2 = 0$, and path loss exponent, $\alpha = 2$, the closed-form expression for the average sum rate can be obtained in the following Corollary.

Corollary 3: A closed-form expression for the average sum rate of NOMA with perfect CSI and path loss factor $\alpha = 2$ is given by (22) shown at the bottom of the page, where C is the Euler's constant, $g(x) = \sum_{p=1}^{j} \binom{j}{p}(-1)^{p+j} e^{\frac{pD^2}{\rho x}} \mathrm{E}_1\left(\frac{pD^2}{\rho x}\right) + \sum_{q=1}^{j}\sum_{p=1}^{j} \binom{j}{p}(-1)^{j-q+p} \frac{(-\frac{pD^2}{\rho x})^q}{(q-1)!} \ln\left(\frac{pD^2}{\rho x}\right), x = a_k, a_{k-1}$.

Proof: See Appendix C. ■

IV. Performance of SOS in NOMA Systems

In this section, the outage probability and the average sum rate of the NOMA systems with only SOS are investigated as follows.

A. Outage Probability

A closed-form expression for the outage performance for different users in NOMA systems, is presented in the following Theorem.

Theorem 3: The outage probability of the k-th nearest user in NOMA protocol, with CSI based on SOS is given by

$$\mathrm{P}_{out,II}^{k} = 1 - 2k\binom{M}{k}\sum_{j=0}^{M-k}\binom{M-k}{j}\frac{(-1)^j}{D^{2(k+j)}} \times \frac{\vec{\eta}^{-\frac{2(k+j)}{\alpha}}}{\alpha}\gamma\left(\frac{2(k+j)}{\alpha}, \vec{\eta}D^{\alpha}\right). \quad (23)$$

Proof: See Appendix D. ■

The diversity order of the users in NOMA systems based on SOS is given in the following Proposition.

Proposition 3: The diversity gain of the k-th nearest user in NOMA systems based on SOS is given by

$$d = -\lim_{\rho\to\infty}\frac{\log \mathrm{P}_{out,II}^{k}}{\log \rho} = 1. \quad (24)$$

Proof: In the high SNR region, i.e., $\rho \to \infty$, and $\vec{\eta} \to 0$, the lower incomplete gamma function in (23) can be written as [26]

$$\gamma\left(\frac{2(k+j)}{\alpha}, \vec{\eta}D^{\alpha}\right) = \sum_{q=0}^{\infty}\frac{(-1)^q(\vec{\eta}D^{\alpha})^{\frac{2(k+j)}{\alpha}+q}}{q!(\frac{2(k+j)}{\alpha}+q)}. \quad (25)$$

From the proposition of $F_{d_k}(x)$ in (51),

$$\lim_{x\to D} F_{d_k}(x) = k\binom{M}{k}\sum_{j=0}^{M-k}\binom{M-k}{j}\frac{(-1)^j}{k+j} = 1. \quad (26)$$

Substituting (25) and (26) into (23), the proof is completed. ■

Note that all users in the above NOMA scheme experience diversity gain equal to one, since small-scale fading will severely deteriorate the outage performance. Similar asymptotic results have been recently obtained in [27] in the context of uplink cloud radio access networks.

B. Average Sum Rate

As mentioned above the joint effect of small-scale fading and large-scale propagation loss are assumed in the channel model. However, in this subsection, the CSI is based on SOS, which means that the channels are ordered by the distance. In this case, we can not always guarantee that the joint channel gain are dominated by distance [19]. For example, there are two users U_1 and U_2 in the cell, with distances, $d_1 \le d_2$. The order of the joint channel gain $|r_1|^2$ and $|r_2|^2$ has two possibilities: $|r_1|^2 \ge |r_2|^2$, and $|r_1|^2 < |r_2|^2$.

It is well known that the SIC depends on the order of the joint channel gain, therefore the NOMA with CSI based on SOS can not assure that a user can remove the signals from the users whose distances are larger than himself with probability one. In general, it seems that it is difficult to obtain a closed-form expression for the average sum rate of NOMA systems, with number of users larger than two. Therefore, we only focus to the case of $M = 2$. In this case, the following approximation of the average sum rate for the whole range of SNR is presented.

Theorem 4: An approximate average sum rate achieved by the NOMA systems is given by (27), shown at the

$$\mathrm{R}_{ave,I} \approx -\sum_{k=1}^{M}\frac{k\binom{M}{k}}{\ln 2}\sum_{r=0}^{k-1}\frac{\binom{k-1}{r}(-1)^r}{r+k}\sum_{j=1}^{r+M-k+1}\binom{r+M-k+1}{j}\left(\frac{-\pi}{nD}\right)^j \sum_{t_1+t_2+\cdots+t_n=j}\frac{j!}{t_1!t_2!\cdots t_n!}\prod_{i=1}^{n}\left(\left|\sin\frac{2i-1}{2n}\pi\right| x_i\right)^{t_i} h(a_k) + \sum_{k=2}^{M}\frac{k\binom{M}{k}}{\ln 2}\sum_{r=0}^{k-1}\frac{\binom{k-1}{r}(-1)^r}{r+k}\sum_{j=1}^{r+M-k+1}\binom{r+M-k+1}{j}\left(\frac{-\pi}{nD}\right)^j \sum_{t_1+t_2+\cdots+t_n=j}\frac{j!}{t_1!t_2!\cdots t_n!}\prod_{i=1}^{n}\left(\left|\sin\frac{2i-1}{2n}\pi\right| x_i\right)^{t_i} h(a_{k-1}). \quad (21)$$

$$\mathrm{R}_{ave,I}^{\sigma_\epsilon^2=0,\alpha=2} = -\sum_{k=1}^{M}\frac{\rho a_k}{\ln 2}\sum_{r=0}^{k-1}\frac{k\binom{M}{k}\binom{k-1}{r}(-1)^r}{r+M-k+1}\sum_{j=1}^{r+M-k+1}\binom{r+M-k+1}{j}\frac{(-1)^j(\rho a_k)^{j-1}}{D^{2j}}\left((-1)^{j+1}\mathrm{C} + g(a_k)\right) + \sum_{k=2}^{M}\frac{\rho a_{k-1}}{\ln 2}\sum_{r=0}^{k-1}\frac{k\binom{M}{k}\binom{k-1}{r}(-1)^r}{r+M-k+1}\sum_{j=1}^{r+M-k+1}\binom{r+M-k+1}{j}\frac{(-1)^j(\rho a_{k-1})^{j-1}}{D^{2j}}\left((-1)^{j+1}\mathrm{C} + g(a_{k-1})\right). \quad (22)$$

bottom of the next page, where $\tau_i = \left(1+\cos\frac{(2i-1)\pi}{2n}\right)$, $x_i = \frac{D}{2}\tau_i$, $x_j = \frac{D}{2}\left(1+\cos\frac{(2j-1)\pi}{2n}\right)$ and n is an approximation parameter of the Gauss-Chebyshev integration, $g_1(y) = \frac{\rho y x_j^{-\alpha+2}}{\left(1+(\frac{\tau_i}{2})^\alpha\right)\ln 2}\exp\left(\frac{x_j^\alpha\left(1+(\frac{\tau_i}{2})^\alpha\right)}{\rho y}\right)\mathrm{E}_1\left(\frac{x_j^\alpha\left(1+(\frac{\tau_i}{2})^\alpha\right)}{\rho y}\right)$, $g_2(y) = \frac{\rho y D^2 x_j^{-\alpha}}{\left(1+(\frac{D\tau_i}{2x_j})^\alpha\right)\ln 2}\exp\left(\frac{x_j^\alpha\left(1+(\frac{D\tau_i}{2x_j})^\alpha\right)}{\rho y}\right)\mathrm{E}_1\left(\frac{x_j^\alpha\left(1+(\frac{D\tau_i}{2x_j})^\alpha\right)}{\rho y}\right)$, $y = 1$, α_1, α_2.

Proof: See Appendix E. ■

Note that if we do not use the Gauss-Chebychev integration to evaluate the average sum rate in Appendix E, the final results of (27) contain double integrals, which will significantly increase the computational complexity. When the Gauss-Chebychev technique is applied, the approximated average sum rate in (27) only depends on the special function exponential integral and the finite-sum of the Gauss-Chebychev integration term. As it can be seen from Section V, a small number of Gauss-Chebyshev integration approximation terms n is used in (27) can match quite well with the Monte Carlo simulations.

C. Outage Probability and Average Sum Rate in OMA Systems

In this subsection, we focus on the outage performance and the average sum rate achieved by the OMA systems with partial CSI. The opportunistic transmission scheme is also considered in the OMA systems, where the rate of U_k with imperfect channel estimation is given by

$$R_k = \frac{1}{M}\log_2\left(1+\frac{|\hat{r}_k|^2}{\sigma_\epsilon^2+\frac{1}{\rho}}\right), k = 1, 2, \ldots, M, \quad (28)$$

and the rate of the k-th nearest user U_k with CSI based on SOS is given by

$$R_k = \frac{1}{M}\log_2\left(1+\rho|r_k|^2\right), k = 1, 2, \ldots, M. \quad (29)$$

Note that we can use (28) and (29) to obtain the outage probability and the average sum rate achieved by OMA. Then these results can be used as benchmarks in order to compare with the NOMA systems in the next Section.

V. Numerical Results and Simulations

In this section, numerical results and Monte Carlo simulations are provided to validate the analytical results presented in this paper. Particularly, the parameters used in the simulations are set as follow. The disk radius is $D = 10\,m$ with the path loss factor, $\alpha = 2, 3, 4$, and the small-scale fading gain is Rayleigh distributed, i.e., $h_i \sim \mathcal{CN}(0, 1)$. The channel estimation error variance σ_ϵ^2 is assumed to take values of 0.005 in Fig. 2, and $\sigma_\epsilon^2 = 0.0001, 0.0005, 0.0008$ in Fig. 3 and 6, respectively. The power allocation factors are $\alpha_k = \frac{2^k-1}{\sum_{l=1}^{M}(2^l-1)}$, $1 \le k \le M$, and the number of Gauss-Chebyshev integral approximation terms is $n = 10$. The Monte Carlo simulation results are averaged over 10^5 independent trials.

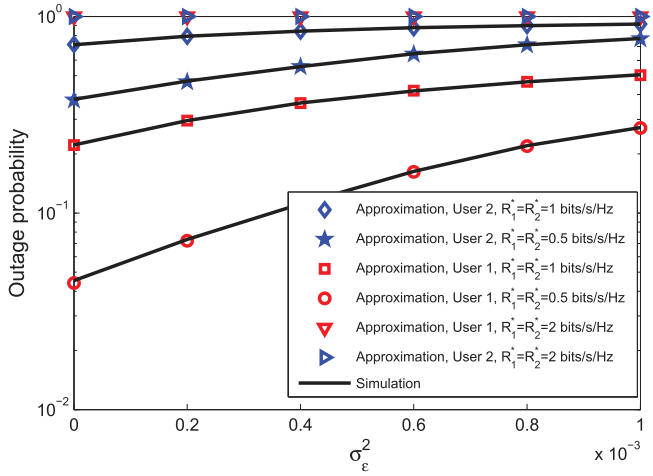

Fig. 1. Outage performance of NOMA based on imperfect CSI with $SNR = 30\,dB$, $\alpha = 3$, and $M = 2$.

In Fig. 1, the analytical results in (10) for the outage performance with imperfect CSI in NOMA systems are shown as a function of the channel estimation error variance σ_ϵ^2. As it can be observed from Fig. 1, the outage performance deteriorates, when increasing the error variance σ_ϵ^2, since higher channel estimation error brings stronger interference. Furthermore, it is worth pointing out that the approximated analytical results in (10) match perfectly with Monte Carlo simulations. In addition, it can be observed from Fig. 1 that when choosing α_i and R_i^* incorrectly, the outage probability will be always 1, since such a choice of the parameters cannot satisfy the condition $\alpha_i > \varepsilon_i \sum_{l=1}^{i-1}\alpha_l$ in Theorem 1.

Fig. 2 illustrates the impact of channel estimation error σ_ϵ^2 on the outage probability in NOMA systems. As observed from Fig. 2, with imperfect CSI, the outage probability floor appears, and NOMA achieves no diversity gain. This is because the channel estimation error ϵ acts as a source of interference. Furthermore, one can observe that NOMA with perfect CSI

$$\mathrm{R}_{\text{ave, II}} \approx \frac{\pi^2}{n^2 D^3}\sum_{i=1}^{n}\tau_i\left|\sin\frac{(2i-1)\pi}{2n}\right|\sum_{j=1}^{n}x_j\left|\sin\frac{(2j-1)\pi}{2n}\right|\left(g_1(\alpha_1)+g_1(\alpha_2)-g_1(1)+g_2(1)-g_2(\alpha_1)-g_2(\alpha_2)\right.$$
$$+\frac{(D^2-x_j^2)\rho\alpha_1 x_j^{-\alpha}}{\ln 2}\exp\left(\frac{x_j^\alpha}{\rho\alpha_1}\right)\mathrm{E}_1\left(\frac{x_j^\alpha}{\rho\alpha_1}\right)\Big) + \frac{2\pi}{nD^3\ln 2}\sum_{i=1}^{n}\left|\sin\frac{(2i-1)\pi}{2n}\right|x_i^3\left(\exp\left(\frac{x_i^\alpha}{\rho}\right)\mathrm{E}_1\left(\frac{x_i^\alpha}{\rho}\right)\right.$$
$$\left.-\exp\left(\frac{x_i^\alpha}{\rho\alpha_1}\right)\mathrm{E}_1\left(\frac{x_i^\alpha}{\rho\alpha_1}\right)\right). \quad (27)$$

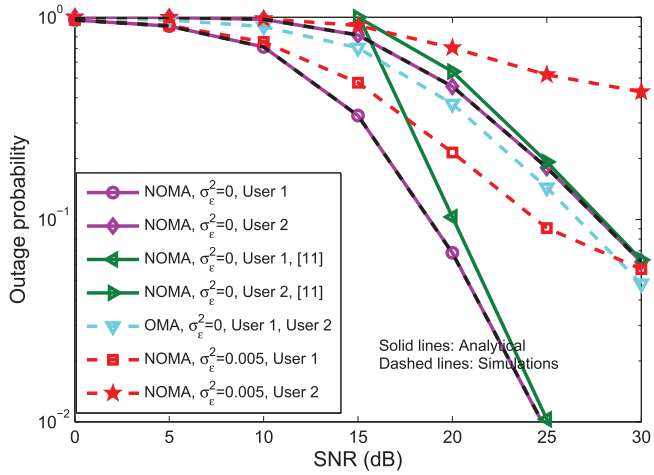

Fig. 2. Impact of σ_ϵ^2 on outage probability, $M = 2$, the targeted rate $R_1^* = R_2^* = 0.5\ bits/s/Hz$, $\alpha = 2$.

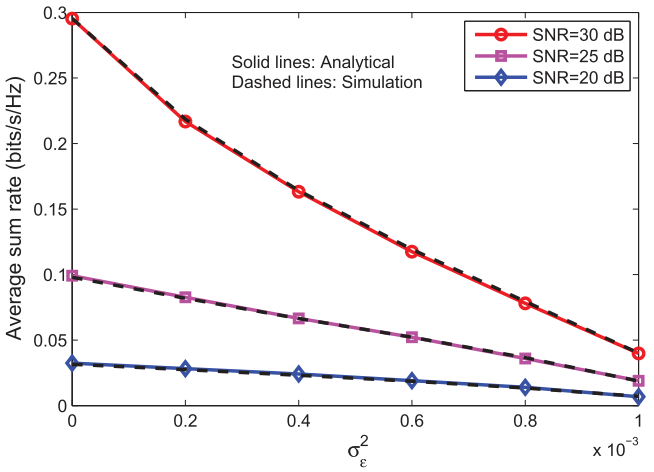

(a) Impact of SNR on average sum rate for different σ_ϵ^2 with $M = 25$.

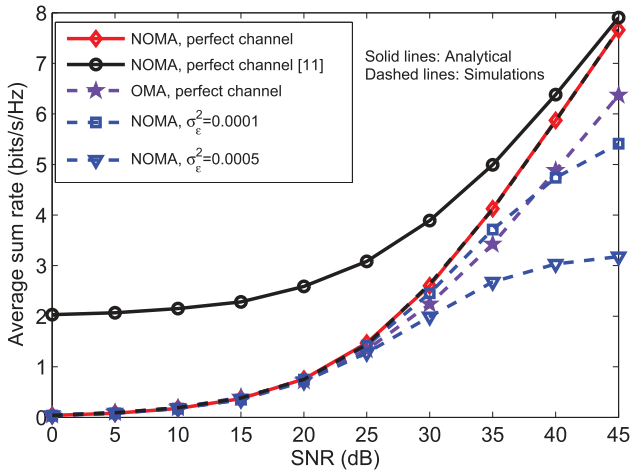

(b) Impact of σ_ϵ^2 on average sum rate with $M = 2$.

Fig. 3. Averaged sum rate of NOMA based on imperfect CSI with $\alpha = 3$.

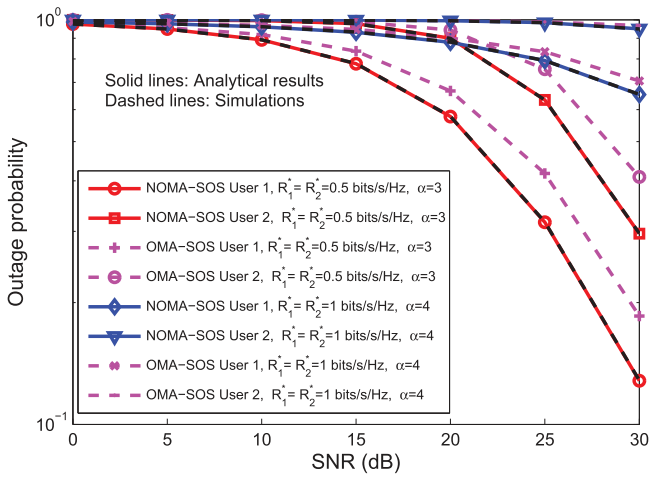

(a) Outage probability analytical results vs Monte Carlo simulations.

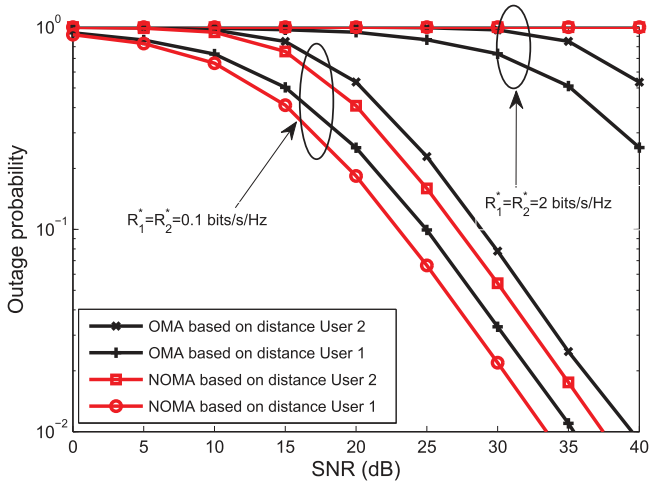

(b) Impact of targeted rate on the outage probability, $\alpha = 3$.

Fig. 4. Outage performance of NOMA based on SOS with two users.

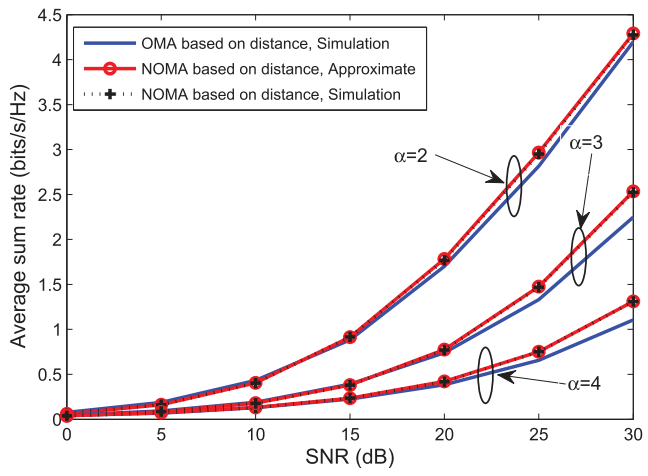

Fig. 5. Average sum rate analytical results vs Monte Carlo simulations, $M = 2$.

achieves a diversity order of $M - k + 1$, while traditional OMA with perfect CSI only achieves a diversity gain of one. In addition, we also compare the analytical results of the NOMA with perfect CSI to those obtained in [11]. As it can be seen from Fig. 2, the approximated results from [11] are accurate only at high SNRs while the analytical results in this paper are close to the Monte Carlo simulations for the whole range of the SNR.

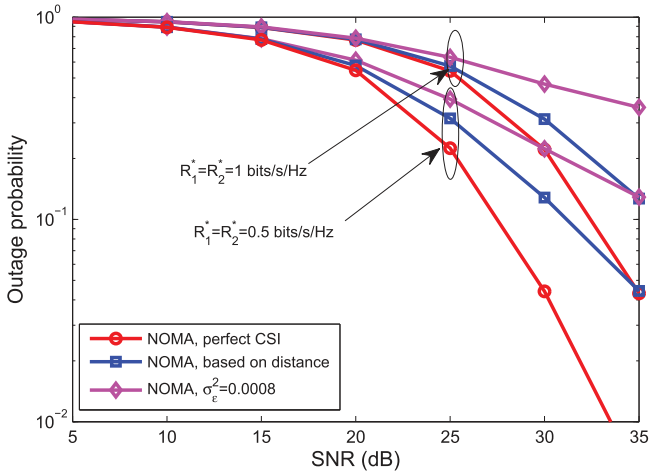

(a) Outage probability of User U_1, $\alpha = 3$.

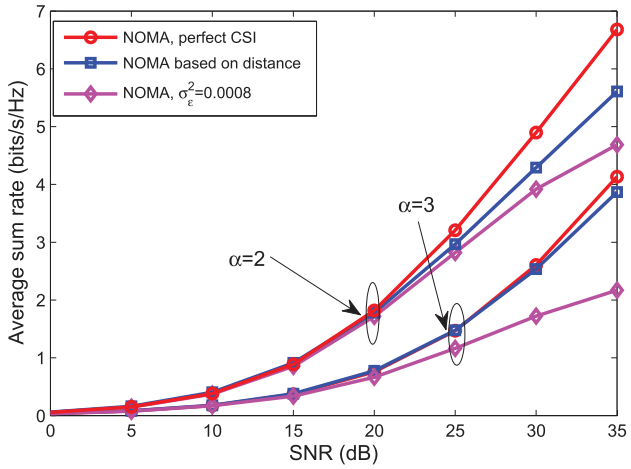

(b) Average sum rate.

Fig. .6 Comparison between the performance of NOMA with imperfect CSI and SOS.

Fig. 3 shows the developed analytical results for the averaged sum rate and compare them to Monte Carlo simulations, in order to show the effect of the channel estimation error variance to the system average sum rate. Fig. 3 demonstrates a perfect match between Monte Carlo simulations and the approximated results, for different channel estimation error variance σ_ϵ^2 and SNR, while the results in [11] only match with Monte Carlo simulations at high SNRs, in the case of NOMA with perfect CSI. Furthermore, the average sum rate of the NOMA protocol based on perfect CSI is superior to OMA scheme, since all the users share the bandwidth resources in NOMA systems at the same time slot. In addition, the worse the channel estimation error is, the poor the achievable average sum rate.

In Fig. 4, we show the approximated analytical results for the outage performance of the SOS based NOMA protocol, by comparing them to the Monte Carlo simulations. It can be observed from Fig. 4 (a) that both NOMA and conventional OMA systems, in which the channels are ordered based on SOS, achieve the same diversity gain, but the former achieves better outage probability than the latter. Once again, the closed-form analytical results in Theorem 3 match quite well with Monte Carlo simulations. Fig. 4 (b) demonstrates that if the parameters R_i^* and α_i are not correctly selected, the users are always failing to detect their own signals.

In Fig. 5, a comparison between the approximate analytical results for the average sum rate in (27) and Monte Carlo simulations is shown. It is evident that the average sum rate of NOMA systems is higher than that of traditional OMA scheme, when both of the channels are ordered based on SOS. Furthermore, the average sum rate decreases when the path loss factor α increases. The reason is that a larger path loss factor can deteriorate the receive SNR, which in turn decreases the average rate. In addition, it is worth pointing out that the approximated analytical results are close to Monte Carlo simulations.

In Fig. 6, we focus on the comparison among different NOMA systems, where the channels are ordered by using imperfect CSI and SOS. As expected, the performance for the case NOMA with CSI based on SOS outperforms that with imperfect CSI. This is because the large-scale path loss distance is a useful information in the channel model, while the channel estimation error, ϵ, is regarded as interference in the systems. In addition, it is interesting to observe that the NOMA with CSI based on SOS can achieve the same performance as the case of perfect CSI at low SNRs. The reason is that the distance dominates the small-scale fading at low SNRs.

VI. Conclusions

In this paper, we have studied the outage probability and the average sum rate for two NOMA schemes, assuming partial CSI. The performance of NOMA with CSI based on SOS are close to that based on perfect CSI at low SNRs, while NOMA with SOS always outperforms NOMA with imperfect CSI. In addition, the analytical expressions demonstrated that the two NOMA protocols can achieve better performance than traditional OMA.

Appendix A
Proof of Theorem 1

Note that the k-th user needs to detect all of the users, whose the estimation channel of their gains are worse than its own. The event that the k-th user successfully decodes the i-th user's message is given by

$$\begin{aligned}\hat{E}_{k,i} &= \left\{ \frac{\alpha_i |\hat{r}_k|^2}{|\hat{r}_k|^2 \sum_{l=1}^{i-1} \alpha_l + \sigma_\epsilon^2 + \frac{1}{\rho}} > \varepsilon_i \right\} \\ &= \left\{ \rho \left(\alpha_i - \varepsilon_i \sum_{l=1}^{i-1} \alpha_l \right) |\hat{r}_k|^2 > \varepsilon_i (\rho \sigma_\epsilon^2 + 1) \right\} \\ &= \left\{ |\hat{r}_k|^2 > \frac{\varepsilon_i (\rho \sigma_\epsilon^2 + 1)}{\rho \left(\alpha_i - \varepsilon_i \sum_{l=1}^{i-1} \alpha_l \right)} \right\}, \end{aligned} \tag{30}$$

where $\varepsilon_i = 2^{R_i^*} - 1$, R_i^* denotes the targeted data rate of the user U_i. The eq. (30) is conditioned on $\alpha_i > \varepsilon_i \sum_{l=1}^{i-1} \alpha_l$.

Therefore the outage probability of the k-th user can be expressed as

$$\begin{aligned}\mathrm{P}_{out,I}^{k} &= 1-\Pr\left\{\bigcap_{i=k+1}^{M}\left(|\hat{r}_k|^2 > \eta_i(\rho\sigma_\epsilon^2+1)\right)\right\}\\ &= 1-\Pr\left\{|\hat{r}_k|^2 > \vec{\eta}(\rho\sigma_\epsilon^2+1)\right\}\\ &= F_{|\hat{r}_k|^2}\left(\vec{\eta}(\rho\sigma_\epsilon^2+1)\right), \end{aligned} \tag{31}$$

where $\eta_i = \frac{\varepsilon_i}{\rho\left(\alpha_i-\varepsilon_i\sum_{l=1}^{i-1}\alpha_l\right)}$, and $\vec{\eta} = \max_{k+1\le i\le M}\eta_i$.

Using order statistics [19], the cumulative distribution function (CDF) of the k-th estimation channel gain $|\hat{r}_k|^2$ can be written as

$$\begin{aligned}F_{|\hat{r}_k|^2}(x) &= k\binom{M}{k}\int_0^{F_{|\bar{r}_k|^2}(x)} t^{M-k}(1-t)^{k-1}dt\\ &= k\binom{M}{k}\sum_{r=0}^{k-1}\binom{k-1}{r}(-1)^r\int_0^{F_{|\bar{r}_k|^2}(x)} t^{r+M-k}dt\\ &= k\binom{M}{k}\sum_{r=0}^{k-1}\binom{k-1}{r}(-1)^r\frac{\left(F_{|\bar{r}_k|^2}(x)\right)^{r+M-k+1}}{r+M-k+1}, \end{aligned} \tag{32}$$

where $F_{|\bar{r}_k|^2}(x)$ is the CDF of the unordered estimation channel gain, which can be evaluated as follows: since the unordered estimate of the channel $r_k = \bar{r}_k + \epsilon$, and $\bar{r}_k \sim \mathcal{CN}(0, d_k^{-\alpha} - \sigma_\epsilon^2)$. Therefore the conditional CDF $F_{|\bar{r}_k|^2|\,d_k}(x|d_k)$ is given by

$$F_{|\bar{r}_k|^2|\,d_k}(z|d_k) = 1-\exp\left(-\frac{z}{d_k^{-\alpha}-\sigma_\epsilon^2}\right). \tag{33}$$

Then,

$$\begin{aligned}F_{|\bar{r}_k|^2}(z) &= \int_0^D F_{|\bar{r}_k|^2|\,d_k}(z|x)\,f_{d_k}(x)dx\\ &= 1-\frac{2}{D^2}\underbrace{\int_0^D x\exp\left(\frac{-z}{x^{-\alpha}-\sigma_\epsilon^2}\right)dx}_{I}. \end{aligned} \tag{34}$$

It is difficult to solve the above integral I, but we can use Gauss-Chebyshev integration [20] to approximate it as

$$I \approx \frac{\pi D}{2n}\sum_{i=1}^{n}\left|\sin\frac{2i-1}{2n}\pi\right| x_i\exp\left(\frac{-z}{x_i^{-\alpha}-\sigma_\epsilon^2}\right), \tag{35}$$

where $x_i = \frac{D}{2}(1+\cos\frac{2i-1}{2n}\pi)$, and n is the number of terms included in the summation.

Recall that the outage probability of the k-th user is $\mathrm{P}_{out}^{k} = F_{|\hat{r}_k|^2}\left(\vec{\eta}(\rho\sigma_\epsilon^2+1)\right)$. Therefore substituting (35) and (34) into (32), the proof is completed.

Appendix B
Proof of Theorem 2

When $R_i^* = R_i$, and based on (4), the average sum rate of NOMA with imperfect CSI can be expressed as

$$\begin{aligned}\mathrm{R}_{\text{ave, I}} &= \mathrm{E}\left[\sum_{k=2}^{M}\log_2\left(1+\frac{\alpha_k|\hat{r}_k|^2}{|\hat{r}_k|^2 a_{k-1}+\sigma_\epsilon^2+\frac{1}{\rho}}\right)\right]\\ &\quad+\mathrm{E}\left[\log_2\left(1+\frac{\alpha_1|\hat{r}_1|^2}{\sigma_\epsilon^2+\frac{1}{\rho}}\right)\right]\\ &= \sum_{k=1}^{M}\underbrace{\mathrm{E}\left[\log_2\left(1+\frac{\rho a_k|\hat{r}_k|^2}{1+\rho\sigma_\epsilon^2}\right)\right]}_{\hat{Q}_k}\\ &\quad-\sum_{k=2}^{M}\underbrace{\mathrm{E}\left[\log_2\left(1+\frac{\rho a_{k-1}|\hat{r}_k|^2}{1+\rho\sigma_\epsilon^2}\right)\right]}_{\hat{V}_k}, \end{aligned} \tag{36}$$

where the average rate of X is defined as

$$\mathrm{E}(X) = \int_{-\infty}^{+\infty}\log_2(1+x)\,f_X(x)dx.$$

From the $F_{|\hat{r}_k|^2}(z)$ in (32), we have

$$\lim_{z\to\infty}F_{|\hat{r}_k|^2}(z) = k\binom{M}{k}\sum_{r=0}^{k-1}\frac{\binom{k-1}{r}(-1)^r}{r+M-k+1} = 1. \tag{37}$$

The $F_{|\hat{r}_k|^2}(z)$ in (32) can be rewritten as

$$\begin{aligned}F_{|\hat{r}_k|^2}(z) \approx 1 + k\binom{M}{k}&\sum_{r=0}^{k-1}\frac{\binom{k-1}{r}(-1)^r}{r+M-k+1}\sum_{j=1}^{r+M-k+1}\binom{r+M-k+1}{j}\\ &\times\left(\frac{-\pi}{nD}\right)^j\underbrace{\left(\sum_{i=1}^{n}\left|\sin\frac{2i-1}{2n}\pi\right| x_i\exp\left(\frac{-z}{x_i^{-\alpha}-\sigma_\epsilon^2}\right)\right)^j}_{Q_{i,n}}. \end{aligned} \tag{38}$$

By using the multinomial Theorem, $Q_{i,n}$ can be further expand as

$$\begin{aligned}Q_{i,n} &= \sum_{t_1+t_2+\cdots+t_n=j}\frac{j!}{t_1!t_2!\cdots t_n!}\\ &\quad\times\prod_{i=1}^{n}\left(\left|\sin\frac{2i-1}{2n}\pi\right| x_i\exp\left(\frac{-z}{x_i^{-\alpha}-\sigma_\epsilon^2}\right)\right)^{t_i}\\ &= \sum_{t_1+t_2+\cdots+t_n=j}\frac{j!}{t_1!t_2!\cdots t_n!}\prod_{i=1}^{n}\left(\left|\sin\frac{2i-1}{2n}\pi\right| x_i\right)^{t_i}\\ &\quad\times\exp\left(-z\sum_{i=1}^{n}\frac{t_i}{x_i^{-\alpha}-\sigma_\epsilon^2}\right). \end{aligned} \tag{39}$$

The expectation $\hat{Q}_k$ in (36) can be evaluated as

$$\hat{Q}_k = \frac{\rho a_k}{\ln 2}\int_0^\infty \frac{1-F_{|\hat{r}_k|^2}(z)}{1+\rho\sigma_\epsilon^2+z\rho a_k}dz$$
$$\overset{(a)}{=} \frac{-\rho a_k k\binom{M}{k}}{\ln 2}\sum_{r=0}^{k-1}\frac{\binom{k-1}{r}(-1)^r}{r+k}\sum_{j=1}^{r+M-k+1}\binom{r+M-k+1}{j}$$
$$\times\left(\frac{-\pi}{nD}\right)^j \sum_{t_1+t_2+\cdots+t_n=j}\prod_{i=1}^{n}\left(\left|\sin\frac{2i-1}{2n}\pi\right| x_i\right)^{t_i}$$
$$\times\frac{j!}{t_1!t_2!\cdots t_n!}\underbrace{\int_0^\infty \frac{\exp\left(-z\sum_{i=1}^n \frac{t_i}{x_i^{-\alpha}-\sigma_\epsilon^2}\right)}{1+\rho\sigma_\epsilon^2+z\rho a_k}dz}_{\hat{Q}_{ki}}, \quad (40)$$

where (a) follows from (38) and (39).

Let $t = 1+\frac{z\rho a_k}{1+\rho\sigma_\epsilon^2}$, the integral $\hat{Q}_{ki}$ in (40) can be evaluated as

$$\hat{Q}_{ki} = \frac{\exp(c_i)}{\rho a_k}\int_1^\infty \frac{\exp(-tc_i)}{t}dt = \frac{\exp(c_i)}{\rho a_k}\mathrm{E}_1(c_i), \quad (41)$$

where $c_i = \frac{1}{\rho a_k}\sum_{i=1}^n \frac{(1+\rho\sigma_\epsilon^2)t_i}{x_i^{-\alpha}-\sigma_\epsilon^2}$, and $\mathrm{E}_1(z) = \int_1^\infty \frac{e^{-zt}}{t}dt$ is exponential integral.

Substituting (41) into (40), the proof $\hat{Q}_k$ is completed. Similarly, we can obtain $\hat{V}_k$. Substituting the results of $\hat{Q}_k$ and $\hat{V}_k$ into (36), the proof is completed.

Appendix C
Proof of Corollary 3

When $\alpha = 2$, by using (37), $F_{|\hat{r}_k|^2}(z)$ in (16) can be expressed as

$$F_{|\hat{r}_k|^2}(z) = 1+\sum_{r=0}^{k-1}\frac{k\binom{M}{k}\binom{k-1}{r}(-1)^r}{r+M-k+1}$$
$$\times\sum_{j=1}^{r+M-k+1}\binom{r+M-k+1}{j}(-1)^j\frac{\left(1-\exp(-zD^2)\right)^j}{D^{2j}z^j}. \quad (42)$$

Similar to (40), $\hat{Q}_k$ in (36) can be evaluated as

$$\hat{Q}_k = \frac{\rho a_k}{\ln 2}\int_0^\infty \frac{1-F_{|\hat{r}_k|^2}(z)}{1+z\rho a_k}dz$$
$$= -\frac{\rho a_k}{\ln 2}\sum_{r=0}^{k-1}\frac{k\binom{M}{k}\binom{k-1}{r}(-1)^r}{r+M-k+1}\sum_{j=1}^{r+M-k+1}\binom{r+M-k+1}{j}$$
$$\times\frac{(-1)^j(\rho a_k)^{j-1}}{D^{2j}}\underbrace{\int_0^\infty\frac{\left(1-\exp(-z\frac{D^2}{\rho a_k})\right)^j}{z^j(1+z)}dz}_{Q_j}. \quad (43)$$

By using partial fractions decomposition and the binomial Theorem,

$$Q_j = \underbrace{\int_0^\infty\left(\frac{(-1)^j}{1+z}+\frac{(-1)^{j-1}}{z}+\sum_{q=2}^{j}\frac{(-1)^{j-q}}{z^q}\right)dz}_{Q_{j1}}$$
$$+\sum_{p=1}^{j}\binom{j}{p}(-1)^{p+j}\int_0^\infty\frac{e^{-zp\frac{D^2}{\rho a_k}}}{1+z}dz$$
$$+\sum_{q=1}^{j}\sum_{p=1}^{j}\binom{j}{p}(-1)^{j-q+p}\underbrace{\int_0^\infty\frac{e^{-zp\frac{D^2}{\rho a_k}}}{z^q}dz}_{Q_{j2}}. \quad (44)$$

The above three integrals can be evaluated as

$$Q_{j1} = -\lim_{z\to 0}\left((-1)^j\ln z+\frac{1}{1-q}\sum_{q=2}^{j}\frac{(-1)^{j-q}}{z^{q-1}}\right), \quad (45)$$

$$\int_0^\infty\frac{e^{-z\frac{pD^2}{\rho a_k}}}{1+z}dz = e^{\frac{pD^2}{\rho a_k}}\mathrm{E}_1\left(\frac{pD^2}{\rho a_k}\right), \quad (46)$$

$$Q_{j2} = \lim_{z\to 0}\sum_{v=1}^{q-1}\frac{(q-v-1)!(-pD^2)^{v-1}e^{-pD^2z}}{(q-1)!z^{q-v}}$$
$$+\lim_{z\to 0}\frac{(-\frac{pD^2}{\rho a_k})^{q-1}}{(q-1)!}\mathrm{E}_1\left(z\frac{pD^2}{\rho a_k}\right), \quad (47)$$

where (46) and (47) follow from [26, (8.211.1)] and [26, (2.324.2)], respectively.

Substituting (45), (46), and (47) into (43), and also using the Taylor series expansion of the exponential integral [26]

$$\mathrm{E}_1\left(z\frac{pD^2}{\rho a_k}\right) = -\mathrm{C}-\ln z-\ln\left(\frac{pD^2}{\rho a_k}\right)-\sum_{k=1}^{\infty}\frac{\left(z\frac{pD^2}{\rho a_k}\right)^k}{kk!},$$

the proof of $\hat{Q}_k$ is completed. Similarly, we can prove $\hat{V}_k$ in (36). Substituting the results of $\hat{Q}_k$ and $\hat{V}_k$ into (36), the result of (22) is obtained.

Appendix D
Proof of Theorem 3

Since SIC is used in the NOMA protocol, the k-th nearest user can detect successfully its own signal only if the k-th nearest user successfully decodes the i-th ($k+1 \le i \le M$) user's signal, where the distance d_i is larger than d_k. After the k-th nearest user can remove these interference signal. The event that the k-th nearest user successfully decodes the i-th nearest user's message is defined as

$$E_{k,i} = \left\{\frac{\alpha_i|r_k|^2}{|r_k|^2\sum_{l=1}^{i-1}\alpha_l+\frac{1}{\rho}} > \varepsilon_i\right\}$$
$$= \left\{|r_k|^2 > \frac{\varepsilon_i}{\rho\left(\alpha_i-\varepsilon_i\sum_{l=1}^{i-1}\alpha_l\right)}\right\}, \quad (48)$$

where the eq. (48) is conditioned on $\alpha_i > \varepsilon_i \sum_{l=1}^{i-1} \alpha_l$.

Therefore the outage probability of the k-th nearest user can be expressed as

$$\begin{aligned} \mathrm{P}_{out,II}^{k} &= 1 - \Pr\left\{ \bigcap_{i=k+1}^{M} \left(|r_k|^2 > \eta_i \right) \right\} \\ &= 1 - \Pr\left\{ |r_k|^2 > \vec{\eta} \right\} \\ &= F_{|r_k|^2}(\vec{\eta}), \end{aligned} \tag{49}$$

where $\eta_i = \frac{\varepsilon_i}{\rho\left(\alpha_i - \varepsilon_i \sum_{l=1}^{i-1} \alpha_l\right)}$, and $\vec{\eta} = \max\limits_{k+1 \le i \le M} \eta_i$.

The CDF of $|r_k|^2$ can be evaluated as follows. Since the locations of the users are uniformly distributed within the disc $\mathcal{D}$, the distance d from an arbitrary user to the BS has the probability distribution function (PDF) and CDF as follows [28]:

$$f_d(x) = \frac{2x}{D^2}, F_d(x) = \frac{x^2}{D^2}, 0 < x \le D. \tag{50}$$

Since $d_1 \le d_2 \le \cdots \le d_M$, by applying order statistics [19], the PDF of the Euclidean distance d_k from the origin to its k-th nearest user as follows:

$$\begin{aligned} f_{d_k}(x) &= k\tbinom{M}{k} (F_d(x))^{k-1} (1 - F_d(x))^{M-k} f_d(x) \\ &= 2k\tbinom{M}{k} \frac{x^{2k-1}}{D^{2k}} \left(1 - \frac{x^2}{D^2}\right)^{M-k} \\ &= 2k\tbinom{M}{k} \sum_{j=0}^{M-k} \tbinom{M-k}{j} (-1)^j \frac{x^{2(k+j)-1}}{D^{2(k+j)}}, \end{aligned} \tag{51}$$

where the binomial coefficient $\binom{N}{n} = \frac{N!}{n!(N-n)!}$.

Since the small-scale Rayleigh fading and large-scale path loss are independent, the CDF of the channel gain $|r_k|^2$ can be evaluated as

$$\begin{aligned} F_{|r_k|^2}(z) &= \Pr\left\{ \frac{|h_k|^2}{d_k^\alpha} \le z \right\} = \int_0^D (1 - e^{-z x^\alpha}) f_{d_k}(x) dx \\ &= 1 - 2k\tbinom{M}{k} \sum_{j=0}^{M-k} \tbinom{M-k}{j} \frac{(-1)^j}{D^{2(k+j)}} \\ &\quad \times \int_0^D e^{-z x^\alpha} x^{2(k+j)-1} dx \\ &= 1 - 2k\tbinom{M}{k} \sum_{j=0}^{M-k} \tbinom{M-k}{j} \frac{(-1)^j}{D^{2(k+j)}} \\ &\quad \times \frac{z^{-\frac{2(k+j)}{\alpha}}}{\alpha} \gamma\left(\frac{2(k+j)}{\alpha}, z D^\alpha\right), \end{aligned} \tag{52}$$

where $\gamma(a, b) = \int_0^b t^{a-1} e^{-t} dt$ is a lower incomplete gamma function [26].

Substituting $\vec{\eta}$ into (52), the proof is completed.

Appendix E
Proof of Theorem 4

When $R_i^* = R_i$, and there are only two users in the disk. The rate of U_1 and U_2 in (9) can be rewritten as

$$R_2 = \log_2\left(1 + \frac{\alpha_2 |r_2|^2}{|r_2|^2 \alpha_1 + \frac{1}{\rho}}\right), \tag{53}$$

and

$$R_1 = \begin{cases} \log_2(1 + \alpha_1 \rho |r_1|^2), & \text{if} |r_1|^2 \ge |r_2|^2; \\ \log_2\left(1 + \frac{\alpha_1 |r_1|^2}{\alpha_2 |r_1|^2 + \frac{1}{\rho}}\right), & \text{otherwise.} \end{cases} \tag{54}$$

Then the average sum rate of the NOMA systems can be expressed as

$$\begin{aligned} \mathrm{R}_{\text{ave, II}} &= \underbrace{\mathrm{E}\left[\log_2(1 + \alpha_1 \rho |h_1|^2 d_1^{-\alpha}) \mid \frac{|h_1|^2}{d_1^\alpha} \ge \frac{|h_2|^2}{d_2^\alpha} \right]}_{Q_1} \\ &\quad + \underbrace{\mathrm{E}\left[\log_2\left(1 + \frac{\alpha_1 |h_1|^2 d_1^{-\alpha}}{|h_1|^2 d_1^{-\alpha} \alpha_2 + \frac{1}{\rho}}\right) \mid \frac{|h_1|^2}{d_1^\alpha} < \frac{|h_2|^2}{d_2^\alpha} \right]}_{Q_2} \\ &\quad + \underbrace{\mathrm{E}\left[\log_2\left(1 + \frac{\alpha_2 |r_2|^2}{|r_2|^2 \alpha_1 + \frac{1}{\rho}}\right) \right]}_{Q_3}. \end{aligned} \tag{55}$$

Since the joint PDF of d_1 and d_2 is $f_{d_1,d_2}(x, y) = \frac{8xy}{D^4}$, $0 < x < y < D$ [19], the expectation Q_1 can be evaluated as

$$\begin{aligned} Q_1 &= \frac{8}{D^4} \int_{x=0}^{D} \int_{u=0}^{\infty} \log_2(1 + \alpha_1 \rho \frac{u}{x^\alpha}) \\ &\quad \times \underbrace{\int_{y=x}^{D} \int_{v=0}^{\frac{u y^\alpha}{x^\alpha}} e^{-v} y dv dy}_{Q_{11}} e^{-u} x du dv. \end{aligned} \tag{56}$$

The double integral Q_{11} in (56) can be calculated as

$$\begin{aligned} Q_{11} &= \int_x^D y \left(1 - e^{-\frac{u y^\alpha}{x^\alpha}}\right) dy \\ &= \frac{D^2}{2} - \frac{x^2}{2} - \frac{x^2}{\alpha u^{\frac{2}{\alpha}}} \gamma\left(\frac{2}{\alpha}, \frac{u D^\alpha}{x^\alpha}\right) + \frac{x^2}{\alpha u^{\frac{2}{\alpha}}} \gamma\left(\frac{2}{\alpha}, u\right). \end{aligned} \tag{57}$$

Substituting (57) into (56), one can observe that the final result of Q_1 contains a double integral, since Q_{11} consists of a lower incomplete gamma function. In order to obtain more insights to Q_1, the Gaussian-Chebyshev integration can be used to approximate the result of Q_{11} in (56) as

$$\begin{aligned} Q_{11} &= \int_x^D y \left(1 - e^{-\frac{u y^\alpha}{x^\alpha}}\right) dy \overset{(a)}{\approx} \frac{\pi}{4n} \sum_{i=1}^{n} \left| \sin \frac{(2i-1)\pi}{2n} \right| \\ &\quad \times \tau_i \left(D^2 - x^2 + x^2 e^{-u \frac{\tau_i^\alpha}{2^\alpha}} - D^2 e^{-u (\frac{D \tau_i}{2x})^\alpha} \right), \end{aligned} \tag{58}$$

where $\tau_i = 1 + \cos \frac{(2i-1)\pi}{2n}$, and (a) follows from Gauss-Chebyshev integration [20].

Substituting (58) into (56), Q_1 can be rewritten as

$$\begin{aligned} Q_1 &= \frac{2\pi}{n D^4} \sum_{i=1}^{n} \tau_i \left| \sin \frac{(2i-1)\pi}{2n} \right| \int_0^D \int_0^\infty \log_2(1 + \frac{\alpha_1 \rho u}{x^\alpha}) \\ &\quad \times \left(D^2 - x^2 + x^2 e^{-u \frac{\tau_i^\alpha}{2^\alpha}} - D^2 e^{-u (\frac{D \tau_i}{2x})^\alpha} \right) e^{-u} du x dx. \end{aligned} \tag{59}$$

Denote the interior integral of Q_1 is Q_{12}, which can be evaluated as

$$\begin{aligned}Q_{12} &= \int_0^\infty \log_2(1+\frac{\alpha_1\rho u}{x^\alpha})\left(D^2 - x^2 + x^2 e^{-u\frac{\tau_i^\alpha}{2^\alpha}} \right.\\ &\quad \left. - D^2 e^{-u(\frac{D\tau_i}{2x})^\alpha}\right) e^{-u} du \\ &= \frac{(D^2-x^2)\rho\alpha_1 x^{-\alpha}}{\ln 2}\int_0^\infty \frac{e^{-u}}{1+\rho\alpha_1 x^{-\alpha}u} du \\ &\quad + \frac{\rho\alpha_1 x^{-\alpha+2}}{\left(1+(\frac{\tau_i}{2})^\alpha\right)\ln 2}\int_0^\infty \frac{e^{-u(1+(\frac{\tau_i}{2})^\alpha)}}{1+\rho\alpha_1 x^{-\alpha}u} du \\ &\quad - \frac{\rho\alpha_1 D^2 x^{-\alpha}}{\left(1+(\frac{D\tau_i}{2x})^\alpha\right)\ln 2}\int_0^\infty \frac{e^{-u(1+(\frac{D\tau_i}{2x})^\alpha)}}{1+\rho\alpha_1 x^{-\alpha}u} du \\ &= \frac{(D^2-x^2)\rho\alpha_1 x^{-\alpha}}{\ln 2}\exp\left(\frac{x^\alpha}{\rho\alpha_1}\right)\mathrm{E}_1\left(\frac{x^\alpha}{\rho\alpha_1}\right) \\ &\quad + \frac{\rho\alpha_1 x^{-\alpha+2}}{b_i\ln 2}\exp\left(\frac{x^\alpha b_i}{\rho\alpha_1}\right)\mathrm{E}_1\left(\frac{x^\alpha b_i}{\rho\alpha_1}\right) \\ &\quad - \frac{\rho\alpha_1 D^2 x^{-\alpha}}{d_i(x)\ln 2}\exp\left(\frac{x^\alpha d_i(x)}{\rho\alpha_1}\right)\mathrm{E}_1\left(\frac{x^\alpha d_i(x)}{\rho\alpha_1}\right), \quad (60)\end{aligned}$$

where $b_i = 1+(\frac{\tau_i}{2})^\alpha$, $d_i(x) = 1+(\frac{D\tau_i}{2x})^\alpha$.

Substributing (60) into (59), and using Gauss-Chebyshev integration [20] again, we can obtain the final result of Q_1 as follows:

$$\begin{aligned}Q_1 &\approx \frac{\pi^2}{n^2 D^3 \ln 2}\sum_{i=1}^n \tau_i \left|\sin\frac{(2i-1)\pi}{2n}\right| \\ &\quad \times \sum_{j=1}^n x_j \left|\sin\frac{(2j-1)\pi}{2n}\right| \left((D^2-x_j^2)\rho\alpha_1 x_j^{-\alpha}\right. \\ &\quad \left. \times \exp\left(\frac{x_j^\alpha}{\rho\alpha_1}\right)\mathrm{E}_1\left(\frac{x_j^\alpha}{\rho\alpha_1}\right) + g_1(\alpha_1) - g_2(\alpha_1)\right), \quad (61)\end{aligned}$$

where $x_j = \frac{D}{2}\left(1+\cos(\frac{(2i-1)\pi}{2n})\right)$.

Similar to Q_1, we can obtain Q_2 as follows:

$$\begin{aligned}Q_2 &\approx \frac{\pi^2}{n^2 D^3}\sum_{i=1}^n \tau_i \left|\sin\frac{(2i-1)\pi}{2n}\right| \sum_{j=1}^n x_j \left|\sin\frac{(2j-1)\pi}{2n}\right| \\ &\quad \times \left(g_2(1) - g_2(\alpha_2) - g_1(1) + g_1(\alpha_2)\right). \quad (62)\end{aligned}$$

The expectation Q_3 in (55) will be evaluated as follows. Let $Z = \frac{\alpha_2|r_2|^2}{\alpha_1|r_2|^2+\frac{1}{\rho}}$, the CDF of Z can be obtained as

$$\begin{aligned}F_Z(z) &= \Pr\left\{\frac{\alpha_2|r_2|^2}{\alpha_1|r_2|^2+\frac{1}{\rho}} < z\right\} \\ &= \Pr\left\{|r_2|^2 < \frac{z}{\rho(\alpha_2-\alpha_1 z)}\right\} \\ &\overset{(a)}{=} 1 - \frac{4}{D^4}\int_0^D x^3 e^{-\frac{zx^\alpha}{\rho(\alpha_2-\alpha_1 z)}} dx \\ &= 1 - \frac{4\rho^{\frac{4}{\alpha}}(\alpha_2-\alpha_1 z)^{\frac{4}{\alpha}}}{\alpha z^{\frac{4}{\alpha}} D^4}\gamma\left(\frac{4}{\alpha}, \frac{z^{\frac{4}{\alpha}} D^\alpha}{\rho^{\frac{4}{\alpha}}(\alpha_2-\alpha_1 z)^{\frac{4}{\alpha}}}\right), \quad (63)\end{aligned}$$

where $0 < z < \frac{\alpha_2}{\alpha_1}$, and (a) follows from (52). If the closed-form expression of $F_Z(z)$ in (63) is used to evaluate the average rate of Q_3 directly, the final result will contain integral expressions. Since the average rate of Q_3 is evaluated as $Q_3 = \int_0^{\frac{\alpha_2}{\alpha_1}} \frac{4\rho^{\frac{4}{\alpha}}(\alpha_2-\alpha_1 z)^{\frac{4}{\alpha}}}{\alpha z^{\frac{4}{\alpha}} D^4(1+z)}\gamma(\frac{4}{\alpha}, \frac{z^{\frac{4}{\alpha}} D^\alpha}{\rho^{\frac{4}{\alpha}}(\alpha_2-\alpha_1 z)^{\frac{4}{\alpha}}})dz$, it is difficult to solve the integral Q_3 which contains a lower incomplete gamma function. In order to obtain Q_3 in closed-from approximation, we apply Gauss-Chebyshev integration [20] to approximate the $F_Z(z)$ as follows:

$$F_Z(z) \approx 1 - \frac{2\pi}{nD^3}\sum_{i=1}^n \left|\sin\frac{(2i-1)\pi}{2n}\right| x_i^3 e^{\frac{-zx_i^\alpha}{\rho(\alpha_2-\alpha_1 z)}}. \quad (64)$$

Now, the expectation Q_3 is evaluated as

$$\begin{aligned}Q_3 &= \frac{1}{\ln 2}\int_0^{\frac{\alpha_2}{\alpha_1}} \frac{1-F_Z(z)}{1+z} dz \\ &= \frac{2\pi}{nD^3\ln 2}\sum_{i=1}^n \left|\sin\frac{(2i-1)\pi}{2n}\right| x_i^3 \underbrace{\int_0^{\frac{\alpha_2}{\alpha_1}} \frac{e^{\frac{-zx_i^\alpha}{\rho(\alpha_2-\alpha_1 z)}}}{1+z} dz}_{Q_{31}}. \quad (65)\end{aligned}$$

Let $t = \frac{zx_i^\alpha}{\rho(\alpha_2-\alpha_1 z)}$, the above integral Q_{31} can be calculated as

$$\begin{aligned}Q_{31} &= \int_0^\infty \frac{\rho\alpha_2 x_i^\alpha e^{-t}}{(\rho t + x_i^\alpha)(\rho\alpha_1 t + x_i^\alpha)} dt \\ &= \int_0^\infty \frac{\rho e^{-t}}{\rho t + x_i^\alpha} dt - \int_0^\infty \frac{\rho\alpha_1 e^{-t}}{\rho\alpha_1 t + x_i^\alpha} dt \\ &= \exp\left(\frac{x_i^\alpha}{\rho}\right)\mathrm{E}_1\left(\frac{x_i^\alpha}{\rho}\right) - \exp\left(\frac{x_i^\alpha}{\rho\alpha_1}\right)\mathrm{E}_1\left(\frac{x_i^\alpha}{\rho\alpha_1}\right). \quad (66)\end{aligned}$$

Substituting (61), (62), (66) and (65) into (55), the proof is completed.

REFERENCES

[1] METIS, "Proposed solutions for new radio access," *Mobile and wireless communications enablers for the 2020 information society (METIS)*, Deliverable D.2.4, Feb. 2015.

[2] 3rd Generation Partnership Project (3GPP), "Study on downlink multiuser superposition transmission for LTE," Shanghai, China, Mar. 2015.

[3] "5G radio access: Requirements, concept and technologies," *NTT DOCOMO, Inc., Tokyo, Japan, 5G Whitepaper*, Jul. 2014.

[4] Y. Saito, A. Benjebbour, Y. Kishiyama, and T. Nakamura, "System level performance evaluation of downlink non-orthogonal multiple access (NOMA)," in *Proc. IEEE Annu. Symp. Pers. Indoor Mobile Radio Commun. (PIMRC)*, London, U.K., Sep. 2013, pp. 611–615.

[5] J. Choi, "Non-orthogonal multiple access in downlink coordinated two-point systems," *IEEE Commun. Lett.*, vol. 18, no. 2, pp. 313–316, Feb. 2014.

[6] Z. Ding, M. Peng, and H. V. Poor, "Cooperative non-orthogonal multiple access in 5G systems," *IEEE* Commun. Lett., vol. 19, no. 8, pp. 1462–1465, Aug. 2015.

[7] M. Al-Imari, P. Xiao, M. A. Imran, and R. Tafazolli, "Uplink non-orthogonal multiple access for 5G wireless networks," in *Proc. 11th Int. Symp. Wireless Commun. Syst. (ISWCS)*, Aug. 2014, pp. 781–785.

[8] Z. Ding, P. Fan, and H. V. Poor, "Impact of user pairing on 5G non-orthogonal multiple access," *IEEE Trans. Veh. Technol.*, 2016, submitted for publication.

[9] P. Xu, Z. Ding, X. Dai, and H. V. Poor, "A new evaluation criterion for non-orthogonal multiple access in 5G software defined networks," *IEEE* Access, vol. 3, pp. 1633–1639, Oct. 2015.

[10] Z. Ding, F. Adachi, and H. V. Poor, "The application of MIMO to non-orthogonal multiple access," *IEEE Trans. Wireless Commun.*, 2016, submitted for publication.

[11] Z. Ding, Z. Yang, P. Fan, and H. V. Poor, "On the performance of non-orthogonal multiple access in 5G systems with randomly deployed users," *IEEE Signal Process. Lett.*, vol. 21, no. 12, pp. 1501–1505, Dec. 2014.
[12] D. Stoyan, W. Kendall, and J. Mecke, *Stochastic Geometry and Its Application*, 2nd ed. Hoboken, NJ, USA: Wiley, 1996.
[13] J. Guo, S. Durrani, and X. Zhou, "Outage probability in arbitrarily-shaped finite wireless networks," *IEEE Trans. Commun.*, vol. 62, no. 2, pp. 699–712, Jan. 2014.
[14] S. Srinivasa and M. Haenggi, "Distance distributions in finite uniformly random networks: Theory and applications," *IEEE Trans. Veh. Technol.*, vol. 59, no. 2, pp. 940–949, Feb. 2010.
[15] S. Timotheou and I. Krikidis, "Fairness for non-orthogonal multiple access in 5G systems," *IEEE Siganl Process. Lett.*, vol. 22, no. 10, pp. 1647–1651, Oct. 2015.
[16] Q. Sun, S. Han, C.-L. I, and Z. Pan, "On the ergodic capacity of MIMO NOMA systems," *IEEE Wireless Commun. Lett.*, vol. 4, no. 4, pp. 405–408, Aug. 2015.
[17] T. Yoo and A. Goldsmith, "Capacity and power allocation for fading MIMO channels with channel estimation error," *IEEE Trans. Inf. Theory*, vol. 52, no. 5, pp. 2203–2214, May 2006.
[18] S. Han, S. Ahn, E. Oh, and D. Hong, "Effect of channel-estimation error on BER performance in cooperative transmission," *IEEE Trans. Veh. Technol.*, vol. 58, no. 4, pp. 2083–2088, May 2009.
[19] H. A. David and H. N. Nagaraja, *Order Statistics*, 3rd ed. Hoboken, NJ, USA: Wiley, 2003.
[20] E. Hildebrand, *Introduction to Numerical Analysis*. New York, NY, USA: Dover, 1987.
[21] S. Ikki and S. Aissa, "Two-way amplify-and-forward relaying with Gaussian imperfect channel estimations," *IEEE Commun. Lett.*, vol. 16, no. 7, pp. 956–959, Jul. 2012.
[22] C. Wang, T.-K. Liu, and X. Dong, "Impact of channel estimation error on the performance of amplify-and-forward two-way relaying," *IEEE Trans. Veh. Technol.*, vol. 61, no. 3, pp. 1197–1207, Mar. 2012.
[23] Y. Ma and J. Jin, "Effect of channel estimation errors on M-QAM with MRC and EGC in Nakagami fading channels," *IEEE Trans. Veh. Technol.*, vol. 56, no. 3, pp. 1239–1250, May 2007.
[24] D. B. H. Cline and G. Samorodnitsky, "Subexponentiality of the product of independent random variables," *Stochastic Process. Appl.*, vol. 49, no. 1, pp. 75–98, Jan. 1994.
[25] D. N. C. Tse, P. Viswanath, and L. Zheng, "Diversity-multiplexing tradeoff in multiple-access channels," *IEEE Trans. Inf. Theory*, vol. 50, no. 9, pp. 1859–1874, Sep. 2004.
[26] I. S. Gradshteyn and I. M. Ryzhik, *Table of Integrals, Series and Products*, 6th ed. New York, NY, USA: Academic, 2000.
[27] M. Peng, S. Yan, and H. V. Poor, "Ergodic capacity analysis of remote radio head associations in cloud radio access networks," *IEEE Wireless Commun. Lett.*, vol. 3, no. 4, pp. 365–368, Aug. 2014.
[28] M. Z. Win, P. C. Pinto, and L. A. Shepp, "A mathematical theory of network interference and its applications," *Proc. IEEE*, vol. 97, no. 2, pp. 205–230, Feb. 2009.

Zheng Yang (S'12) received the B.S. degree in mathematics from Minnan Normal University, Zhangzhou, China, and the M.S. degree in mathematics from Fujian Normal University, Fuzhou, China, in 2008 and 2011, respectively. He is currently pursuing the Ph.D. degree at the Institute of Mobile Communications, Southwest Jiaotong University, Chengdu, China. He was a Visiting Ph.D. Student at the School of Electrical and Electronic Engineering, Newcastle University, Newcastle upon Tyne, U.K., from January 2014 to July 2014. His research interests include 5G networks, co-operative and energy harvesting networks, signal design, and coding.

Zhiguo Ding (S'03–M'05–SM'15) received the B.Eng. in electrical engineering from the Beijing University of Posts and Telecommunications, Beijing, China, and the Ph.D degree in electrical engineering from Imperial College London, London, U.K., in 2000 and 2005, respectively. From July 2005 to August 2014, he was working with Queen's University Belfast, Belfast, U.K., Imperial College London, and Newcastle University, Newcastle upon Tyne, U.K. Since September 2014, he has been with Lancaster University, Lancaster, U.K., as a Chair Professor. From October 2012 to September 2016, he was an Academic Visitor at Princeton University, Princeton, NJ, USA. His research interests include 5G networks, game theory, co-operative and energy harvesting networks, and statistical signal processing. He is serving as an Editor for the IEEE TRANSACTIONS ON COMMUNICATIONS, the IEEE TRANSACTIONS ON VEHICULAR TECHNOLOGY, the IEEE WIRELESS COMMUNICATION LETTERS, the IEEE COMMUNICATION LETTERS, and the *Journal of Wireless Communications and Mobile Computing*. He was the recipient of the best paper award in IET Communication Conference on Wireless, Mobile and Computing, 2009, the IEEE Communication Letter Exemplary Reviewer 2012, and the EU Marie Curie Fellowship 2012–2014.

Pingzhi Fan (M'93–SM'99–F'15) received the Ph.D. degree in electronic engineering from the Hull University, Kingston upon Hull, U.K. He is currently a Professor and the Director of the Institute of Mobile Communications, Southwest Jiaotong University, Chengdu, China. He has had over 200 research papers published in various academic English journals (IEEE, IEE, and IEICE), and eight books, and is the inventor of 22 granted patents. His research interests include high mobility wireless communications, 5G technologies, wireless networks for big data, signal design, and coding. He is an IEEE VTS Distinguished Lecturer (2015–2017), and a Fellow of IET, CIE, and CIC. He served as General Chair or a TPC Chair of a number of international conferences, and is the Guest Editor-in-Chief, the Guest Editor or the Editorial Member of several international journals. He is the Founding Chair of the IEEE VTS BJ Chapter, the IEEE ComSoc CD Chapter, and the IEEE Chengdu Section. He also served as a Board Member of IEEE Region 10, IET (IEE) Council and IET Asia-Pacific Region. He was the recipient of the U.K. ORS Award, the Outstanding Young Scientist Award by NSFC, and the Chief Scientist of a National 973 Research Project.

George K. Karagiannidis (M'96–SM'03–F'14) was born in Pithagorion, Samos Island, Greece. He received the University Diploma and Ph.D. degrees in electrical and computer engineering from the University of Patras, Patras, Greece, in 1987 and 1999, respectively. From 2000 to 2004, he was a Senior Researcher with the Institute for Space Applications and Remote Sensing, National Observatory of Athens, Athens, Greece. In June 2004, he joined the Faculty of Aristotle University of Thessaloniki, Thessaloniki, Greece, where he is currently a Professor of electrical and computer engineering and the Director of Digital Telecommunications Systems and Networks Laboratory. He is an Honorary Professor with Southwest Jiaotong University, Chengdu, China. His research interests include digital communication systems with emphasis on wireless communications, optical wireless communications, wireless power transfer and applications, molecular communications, communications and robotics, and wireless security. He is the author or coauthor of more than 400 technical papers published in scientific journals and presented at international conferences. He is also the author of the Greek edition of a book, *Telecommunications Systems* and coauthor of the book, *Advanced Optical Wireless Communications Systems* (Cambridge Publications, 2012). He has been selected as a 2015 Thomson Reuters Highly Cited Researcher. He has been involved as the General Chair, the Technical Program Chair and a member of technical program committees in several IEEE and non-IEEE conferences. In the past, he was an Editor of the IEEE TRANSACTIONS ON COMMUNICATIONS, a Senior Editor of the IEEE COMMUNICATIONS LETTERS, an Editor of the *EURASIP Journal of Wireless Communications and Networks*, and several times a Guest Editor of the IEEE SELECTED AREAS IN COMMUNICATIONS. From 2012 to 2015, he was the Editor-in Chief of the IEEE COMMUNICATIONS LETTERS.